geographical analysis

Geographical Analysis (2024) **56**, 600–623

An Efficient Solving Approach for the *p*-Dispersion Problem Based on the Distance-Based Spatially Informed Property

Changwha Oh[1], Hyun Kim[1], and Yongwan Chun[2]

[1]Department of Geography and Sustainability, University of Tennessee at Knoxville, Knoxville, Tennessee, USA, [2]School of Economic, Political and Policy Sciences, The University of Texas at Dallas, Richardson, Texas, USA

The p-*dispersion problem is a spatial optimization problem that aims to maximize the minimum separation distance among all assigned nodes. This problem is characterized by an innate spatial structure based on distance attributes. This research proposes a novel approach, named the* distance-based spatially informed property *(D-SIP) method to reduce the problem size of the* p-*dispersion instances, facilitating a more efficient solution while maintaining optimality in nearly all cases. The D-SIP is derived from investigating the underlying spatial characteristics from the behaviors of the* p-*dispersion problem in determining the optimal location of nodes. To define the D-SIP, this research applies Ripley's* K-*function to the different types of point patterns, given that the optimal solutions of the* p-*dispersion problem are strongly associated with the spatial proximity among points discovered by Ripley's* K-*function. The results demonstrate that the D-SIP identifies collective dominances of optimal solutions, leading to building* the spatially informed p-dispersion model. *The simulation-based experiments show that the proposed method significantly diminishes the size of problems, improves computational performance, and secures optimal solutions for 99.9% of instances (999 out of 1,000 instances) under diverse conditions.*

Introduction

Spatial optimization and spatial statistics are major research areas with applications in geography, location science, mathematics, statistics, and Geographic Information Science. Despite the interdisciplinary nature of the intersection among these disciplines, there has been a lack of a synergistic research interface (Griffith, Chun, and Kim 2022). While some recent attempts have been made to explore the relationship between spatial association and spatial optimization and integrate them into a holistic framework (Griffith 2021; Griffith, Chun, and Kim 2022, 2023), these efforts have been limited in their focus on uncovering the potential of spatial association to improve the solution efficiency of location-allocation problems, such as the *p*-median location problem.

Correspondence: Hyun Kim, Department of Geography and Sustainability, University of Tennessee at Knoxville, 1000 Philip Fulmer Way, Knoxville, TN 37996-0925, USA
e-mail: hkim56@utk.edu

Submitted: July 23, 2023. Revised version accepted: January 30, 2024.

doi: 10.1111/gean.12392

Spatial optimization problems have a model structure that is naturally articulated with spatial association in input metrics such as locations of nodes, and the proximity among nodes in a space in finding the optimal solutions. For example, Griffith, Chun, and Kim (2022) highlight that spatial autocorrelation plays an important role in solving spatial optimization problems, particularly the *p*-median location problem, through three distinct mechanisms: (1) helping to reduce solution spaces to solve the problem efficiently, (2) initializing solutions that can lead to optimal (or near-optimal) solutions effectively when heuristic methods are considered, and (3) improving solution quality through imputations of missing attributes on nodes. The fundamental decision process of the *p*-median location problem is to determine the optimal allocations of *p*-facilities that minimize the total weighted sum of attributes. The Mixed Integer Programming (MIP) formulation of the problem requires attributes on each node, such as weights (w) at demands and distances (d) among them or from demand nodes to potential facility sites. The well-known critical issue is its solving capability because of the complexity of the problems, often known as *NP-hard*. As an alternative perspective, Mei et al. (2022) utilize spatial information derived from underlying point patterns to approximate optimal solutions for the vehicle routing problem (VRP). They demonstrate how leveraging complementary spatial information can enhance the outcomes of specific types of spatial optimization problems.

The efforts to reduce the computational burden of this decision process have been focused on the methods, including removing decision variables, reformulating the problem structure from the MIP form (Church 2003), or narrowing the search space of candidate facility sites (Lei and Church 2015). In contrast, Kim, Chun, and Griffith (2019) propose an idea to use unique behaviors of the spatial optimization model's solutions which are influenced by the underlying spatial characteristics among demands or candidate facilities, and they can be explicitly embedded in the model building process as a form of constraints or alternative attributes to lower the complexity of the problems, which is defined as *spatially informed property* (SIP).

However, unlike other spatial optimization problems, the *p*-dispersion problem depends solely on the distance property, indicating that a potential SIP can be driven based on the distances among nodes to select *p*-dispersed facilities. The *p*-dispersion problem aims to identify the locations of *p*-facilities that maximize the minimum separation distance among facilities, considering the distances among nodes (Shier 1977; Kuby 1987). This problem is classified as *NP-hard*, indicating the problem becomes quickly intractable to identify optimal solutions via mathematical programming (Erkut 1990). In this research, we propose a SIP approach named *the distance-based spatially informed property* (D-SIP) to effectively solve the *p*-dispersion models. The D-SIP is defined as the extent of influence that the distances between each node and all other nodes exert on the probability of a node being part of an optimal solution, where each node is a potential facility location with an associated location decision variable. Consequently, the D-SIP provides a basis to discern which decision variables are essential or non-essential in finding the optimal solutions. To enable the D-SIP for the *p*-dispersion problem in a systematic manner, we examine how the D-SIP varies across different spatial point patterns, with the assumption that the degree of influence is related to the level of *clustering* among nodes.

The relationship between the D-SIP and the behavior of the optimal solutions in the *p*-dispersion problem is examined by conducting numerical simulations on spatial point patterns of nodes, with specifically controlled settings. By leveraging the D-SIP, the conventional *p*-dispersion problem is reformulated in mathematical MIP formulation as the *spatially informed p-dispersion* (*SI-dispersion*) *model* by eliminating non-essential decision variables from the original model, demonstrating improved solution capability while guaranteeing optimality. The knowledge gained from the revealed D-SIP helps to improve the model's capacity to solve the p-dispersion problem without compromising the quality of solutions and provides a foundation to develop an efficient approach to solving any spatial optimization problems related to the dispersion of facilities.

Background and literature

The p-dispersion problem is a spatial optimization problem that involves finding the optimal locations for p facilities to maximize the minimum distance between any pair of facilities. The problem is particularly useful for locating hazardous or obnoxious facilities, such as nuclear silos, landfills, or franchise outlets, in order to minimize a concentration of potential risks to surrounding communities or prevent any potential chain reaction among facilities such as the explosion of nuclear facilities. By optimizing facility locations, potential negative impacts can be spread out or prevented, making the problem a valuable tool in spatial planning and risk management (Daskin 2013).

The concept of the p-dispersion problem was first recognized by Shier (1977). Shier showed that the p-dispersion problem and the $(p-1)$ center problem exhibit a duality relationship on tree networks. This duality implies that the optimal solution (i.e., a minimum of the maximum separation distance) for the p-center problem is equal to half of the optimal solution for the p-dispersion problem. Subsequently, several studies considered the dual relationship between p-dispersion problems and p-center problems on tree networks and attempted to solve the problems using various solution techniques, including nonlinear approaches and heuristic algorithms (Chandrasekaran and Daughety 1981; Chandrasekaran and Tamir 1982; Tansel et al. 1982; Chaudhry, McCormick, and Moon 1986). Chandrasekaran and Daughety (1981) developed polynomial time algorithms for solving both the dispersion problem and the center problem, by solving a finite series of cover problems and anti-covering problems (i.e., opposite to the cover problem, which aims to locate the maximum number of facilities with sufficient distance from each other), respectively. Similarly, the other papers also utilized the concept of cover and anti-covering approaches to solve center problems and dispersion problems based on the duality relationship.

Kuby (1987) first formally presented a MIP formulation for the p-dispersion problem. The MIP formulation for the p-dispersion problem is classified as *NP-hard* due to the sizable combinatorial increase in decision variables, which leads to a rapid deterioration in its solvability (Erkut 1990; Ghosh 1996). However, researchers have observed that many decision variables in the model are unnecessary under certain values of p (Curtin and Church 2006, 2007). Therefore, if it is possible to identify and remove these unnecessary decision variables from the model systematically, computational efficiency will be enhanced, likely enabling exact solution procedures to solve larger instances to optimality and allowing heuristic procedures to find optimal or near-optimal solutions more quickly. The standard MIP formulation of the p-dispersion problem is expressed as follows:

$$\textit{Maximize } D \tag{1}$$

Subject to

$$\sum_i Y_i = p \tag{2}$$

$$D \le d_{ij} + M\left(2 - Y_i - Y_j\right) \quad \forall i,j,\ \ j > i \tag{3}$$

$$Y_i \in \{0, 1\} \quad \forall i \tag{4}$$

where D: the smallest separation distance between any pair of open facilities, Y_i: 1 if a facility locates at node i, 0 otherwise, M: a very large number, d_{ij}: distance between node i and j, and p: the number of open facilities.

The objective function (1) of the p-dispersion problem is to maximize the minimum separation distance D between a pair of open nodes. Constraint (2) defines that p-facilities should be determined. Constraint (3) stipulate that the minimum distance between the two nearest open facilities should be maximized. In constraint (3), if both nodes i and j are selected as open facilities, then the objective function D should be less than or equal to the separation distance between node i and j (d_{ij}). This condition ensures that the objective function D represents the smallest separation distance among all separation distances between two open facilities. Constraint (4) impose integer restrictions on the decision variables.

While the structure of the p-dispersion problem's formulation appears intuitive, solving it as a MIP poses considerable computational demands. As highlighted by Kuby (1987), the p-dispersion problem does not necessitate the calculation of all integer solutions due to potential pruning of branch-and-bound trees. Nonetheless, the problem is not "integer-friendly", and the number of decision variables significantly influences the number of potential feasible solutions. Consequently, even small instances of the problem can incur a substantial growth of their complexity. For instance, the solution complexity could reach $O(n^2)$ with n input nodes, primarily due to the exponential growth of the number of constraints (3) (Sayyady and Fathi 2016). To tackle this challenge, several methods have been addressed, including (1) exploring unnecessary decision variables to be removed (Curtin and Church 2006; Contardo 2020), (2) reformulating the model to make the problem more compact (Kuo, Glover, and Dhir 1993; Sayyady and Fathi 2016; Sayah and Irnich 2017), or (3) tightening the solution space by identifying good bounds (Pisinger 2006); all of them thereby focus on mitigating the complexity of the model.

Curtin and Church (2006) introduced the neighborhood constraint elimination method, which reduces the size of the problem by exploiting the idea that ($p-2$)-farthest nodes from each node do not need to be considered as optimal solutions because these pairs are always shorter than p-farthest and ($p-1$)-farthest nodes. Contardo (2020) proposed a decremental clustering method to reduce the problem size while guaranteeing optimality. The idea of the algorithm is to divide input nodes into several clusters using a k-means clustering algorithm. The algorithm forms p clusters, and the maximum separation distance between a pair of nodes from two different clusters serves as an upper bound of the original p-dispersion problem. The algorithm iteratively refines clusters by dividing them into two ($k=2$) smaller clusters when the maximum separation distance between a pair of nodes within a cluster exceeds the lower bound of the original problem. The algorithm continues until the clusters are sufficiently refined, meaning that the maximum separation distance between any pair of nodes from two different clusters becomes smaller than the optimal solution of the given p-dispersion problem. This approach serves as a bounding technique that enables finding exact solutions designed for solving the dispersion problem.

Kuo, Glover, and Dhir (1993) formulated the maximin diversity problem, which shares a similar underlying idea to the p-dispersion problem but was designed to address situations where diversifying p clusters based on the characteristics of elements is a crucial consideration in optimal solutions. The problem provided the flexibility to employ additional decision variables for the links between two open facilities (such as X_{ij}), which might tighten the solution space, although the method can result in a sizeable number of extra constraints compared to the model by Kuby (1987). Meanwhile, Sayyady and Fathi (2016) proposed an alternative exact solution approach that exploits the relationship between the p-dispersion problem and the node packing problem, also known as the anti-covering location problem. The core idea behind their approach is based on the similarities between the two models in their pursuit of finding optimal solutions. The objective of the node packing problem is to maximize the number of nodes such that no two nodes are adjacent to each other, considering a given distance criteria. The procedure that they introduced for solving the p-dispersion problem involves solving the node packing problem with different criteria through binary search. The search continues simply until the objective value of the node packing problem reaches the number of open facilities (p). By leveraging the relative ease of solving the node packing problem compared to the p-dispersion problem, and the efficient nature of the binary search in reducing the number of iterations, their approach efficiently tackles large-size problems while guaranteeing optimality.

Parreño, Álvarez-Valdés, and Martí (2021) made further enhancements to the procedure proposed by Sayyady and Fathi (2016). They introduced additional constraints to the node packing problem, specifically stipulating the number of facilities to be located. The modified model was then just submitted to an optimization solver to confirm its feasibility. This modification makes the performance of the solution procedure faster compared to the original method. Sayah and Irnich (2017) introduced a compact formulation for the p-dispersion problem. Their approach involves deriving unique distance values from the distance matrix among nodes. The concept of unique distances is rooted in the characteristic that an optimal solution to the p-dispersion problem always corresponds to a distinct distance value within the unique distance set. The set comprises distance values among all pairs of nodes, ensuring that none are identical to another. Their formulation introduces additional integer decision variables, which determine whether the solution exceeds one of the unique distances from all possible separation distances. If the decision variable that is associated with a certain unique distance value equals 1 (selected), then the objective value should be greater than or equal to that unique distance. By adopting this specification, their approach reduces the number of constraints involved potentially, resulting in compacting the size of the problems. Finally, Pisinger (2006) developed methods that use Lagrangian relaxation and semidefinite programming to find and tighten the upper bounds for the p-dispersion problem. The acquired upper bounds from both methods successfully reduce the size of the solution space.

The SI-dispersion model distinguishes itself from previous attempts because it is rooted in the idea of SIP to solve spatial optimization problems. As an alternative but promising method, the SIP-based MIP approach significantly reduces solution times and maintains the quality of solutions (i.e., optimality), especially in the case of the class of p-dispersion problems. As drawn from the previous discussion on the SIP, distinguishing between essential and non-essential decision variables serves as a fundamental step in model formulation, particularly in spatial optimization problems. The underlying assumption is that non-essential decision variables, due to their redundancy, exacerbate the complexity of the model and the quality of a solution (Griffith, Chun, and Kim 2022). Given this, systematically eliminating these variables from the model formulation is crucial in reducing the problem size of the p-dispersion problem. To develop a SIP approach, developing measurable spatial information as a criterion is the key, which can discern essential and non-essential decision variables (usually 0–1 decision variables) in the MIP model. As SIP for the p-dispersion problem, we employ a local measurement of Ripley's K-function (Ripley 1976, 1977) to derive the spatial information. Since the p-dispersion problem uses the distance property as a *single attribute* only to find optimal solutions, Ripley's K-function is suitable as SIP because it is a distance-based method using distance as a sole attribute. Thereby, it is convenient to explore systematically the SIP as a criterion that can be used for the elimination or conservation of the decision variables for the *p*-dispersion problem. In addition, Ripley's *K*-function not only provides spatial information but also serves as a framework for deriving the SIP for different types of point patterns. This function has been widely used in point pattern analysis (O'Sullivan and Unwin, 2010), making it a suitable measurement for capturing the SIP given the distribution of points.

To discover the characteristics of SIP and develop the SI-dispersion model, a course of simulation experiments was designed based on the type of point pattern of the *p*-dispersion problem. The simulation experiments aim to leverage the fact that the *p*-dispersion problem is solely concerned with the "distance" spatial property, that is, D-SIP. The objective was to gain insights into how effectively this property is incorporated into the model-building process. Key measurements regarding model performance, such as the number of decision variables in the model, the number of branch-and-cuts, and solution times, were used in the evaluation.

Research design: Simulation experiments

Principle to drive D-SIP

Since D-SIP should work as a criterion to distinguish essential and non-essential decision variables in any problem instances, a single measure quantified by their proximity among nodes would be beneficial. In essence, the D-SIP determines the likelihood of a node being included in an optimal solution by exploiting the spatial relativeness of a node with other nodes in a study area. Under this assumption, this research considers Ripley's local *K*-function to drive D-SIP. The function is a class of spatial association measurements to capture the second-order effect at the individual node level, allowing us to gauge the spatial relativeness of a node from the distance-based point pattern of nodes using a specific bandwidth that is relevant to the point patterns under consideration (Ripley 1976; Getis and Franklin 1987; O'Sullivan and Unwin 2010). With this property, we define the D-SIP as a value for node i obtained from Ripley's local *K*-function, $L_i(d)$ with a bandwidth distance d in n nodes space. The $L_i(d)$ is calculated using Equation (5) below.

$$L_i(d) = \sqrt{\frac{A \sum_{j=1}^{n} k_{ij}}{\pi(n-1)}} \tag{5}$$

where k_{ij}: 1 if $d_{ij} \le d$, or 0 otherwise, d_{ij}: distance between node i and j, d: search bandwidth distance, n: the number of nodes, and A: an area of spatial extent.

Equation (5) indicates that the value of $L_i(d)$, the relative influence of spatial association by distance (d_{ij}) of node i, is determined by the number of neighboring nodes j in the search bandwidth (d) and the spatial extent A. Notice that the area of extent A is a constant, thus its impact is also constant with nodes. However, the $L_i(d)$ varies with what bandwidth distance (d) is defined, because $L_i(d)$ is influenced by the number of k_{ij} identified within the bandwidth and their proximities to node i. In general, the greater number of neighborhood nodes j identified within the bandwidth for node i, the greater $L_i(d)$ is expected, posing a stronger influence on the spatial association of node i with its neighboring nodes.

Fig. 1 shows two major behaviors of the relationships between $L_i(d)$ with bandwidth d of two sample nodes in a square space, portrayed in the perspective by the location where one is located at the extreme corner and the other is centered (Fig. 1a), and by a different density

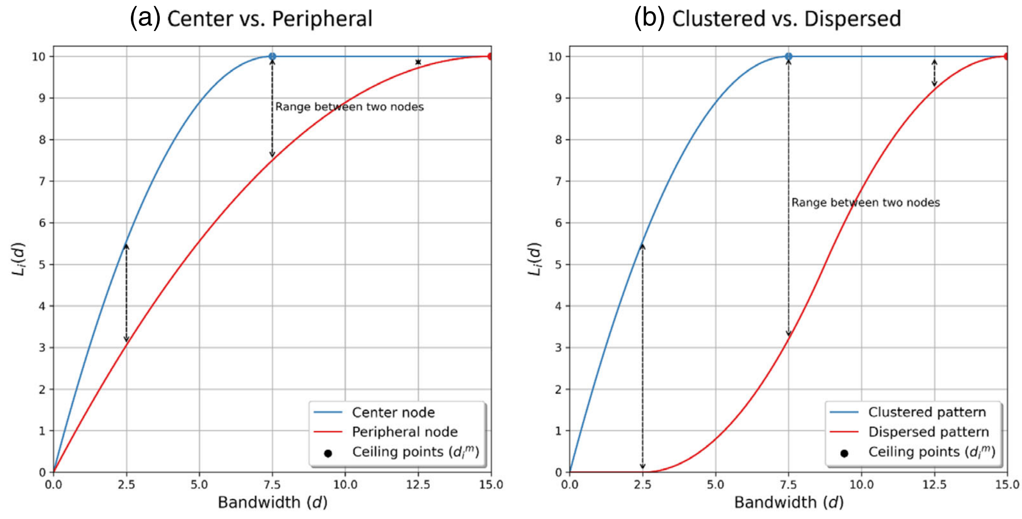

Figure 1. Relationships between $L_i(d)$ and incremental bandwidth d by (a) different locations of nodes (center vs. peripheral) and (b) a center node under the different spatial patterns (clustered vs. dispersed).

(clustered vs. dispersed) for a centered node (Fig. 1b). For discussion, the resulting relationships between $L_i(d)$ and d are smoothed on purpose. Several observations are worth highlighting to drive the D-SIP. First, $L_i(d)$ of a node (y-axis) increases along with an increase of bandwidth d (x-axis) because a greater bandwidth may include more neighboring nodes j in the computation for node i. Theoretically, any node i will eventually reach the maximal value of $L_i(d)$ (i.e., the ceiling point) at a certain moment as d increases. However, the rates at which they reach the point are different, depending on the location of a node relative to other nodes as well as the spatial patterns of nodes in space. In detail, as demonstrated in Fig. 1a, a node located centrally in a space reaches the maximal $L_i(d)$ quickly compared to a node in a peripheral area. In terms of spatial pattern, a node in a clustered area exhibits a steeper increase in $L_i(d)$ compared to a node in a sparse area, though both will eventually reach the maximal $L_i(d)$ when they include all other nodes within the bandwidth. Second, from the perspective of the distribution of the values of $L_i(d)$, notice that the bandwidth also affects the ranges of $L_i(d)$ (=max $L_i(d)$ − min $L_j(d)$ by d). As shown in Fig. 1a,b, the gaps in $L_i(d)$ between two sample nodes are hardly noticeable at small bandwidths. However, the gaps gradually increase until the maximal $L_i(d)$ with an incremental increase in bandwidth is reached by a node, followed by narrower ranges of $L_i(d)$ after surpassing the maximal $L_i(d)$ and the $L_i(d)$ values of nodes converge to the maximal $L_i(d)$ at the end. Of critical concern is how to find the ideal bandwidth to derive the best D-SIP to be used as a criterion to be embedded in solving the p-dispersion problem instances.

As discussed in previous sections, classifying decision variables in spatial optimization problems as either essential or non-essential is crucial in reducing problem complexity. The $L_i(d)$ value assigned to each node plays a pivotal role in determining essential or non-essential decision variables in the p-dispersion problems. It is important to highlight that a wider range of $L_i(d)$ values across the nodes within the research space ensures a greater level of differentiation among them, providing more definitive and robust criteria for identifying whether a node qualifies as an essential or non-essential decision variable.

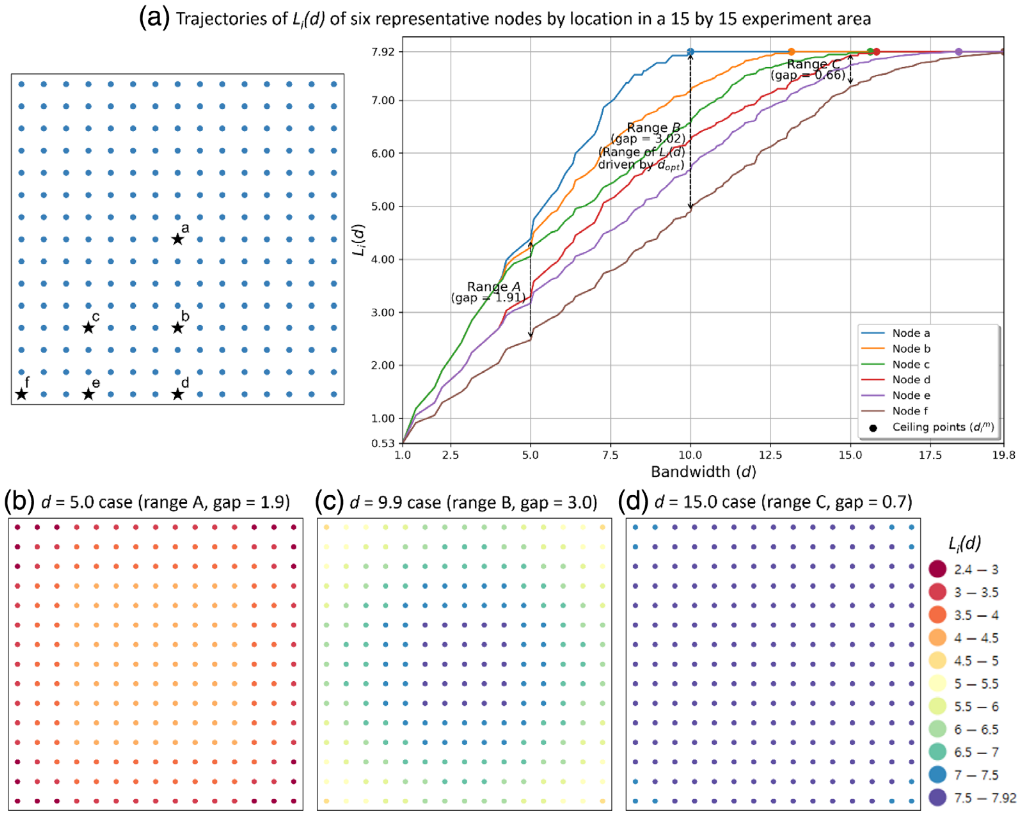

Figure 2. The simulation experiments of the $L_i(d)$ by locations with incremental bandwidth and the pattern of $L_i(d)$ by different bandwidths d, (b) $d = 5.0$ case, (c) $d = 9.9$ case, and (d) $d = 15.0$ case. "gap" in (b), (c), and (d) means the difference between the largest and the smallest $L_i(d)$ value from the given set of nodes *a*–*f*.

To illustrate this, Fig. 2 details the simulation experiments showing the trajectories of $L_i(d)$ with incremental bandwidths d for a 15 by 15 gridded square area with 225 nodes one distance unit apart. The experiments are performed to elucidate the general behaviors of $L_i(d)$ to determine the ideal bandwidth d for the D-SIP simulation. Exploring the $L_i(d)$ trajectories for nodes at different locations within the study area allows us to effectively determine the ideal bandwidth d for the D-SIP simulation in solving the *p*-dispersion problems. It is important to note that we conducted these experiments with a 15 by 15 gridded square area because it offers a more controlled environment for validating our approach. For the convenience of visual investigation, Fig. 2a displays six representative nodes in a quadrant of the study area by their locations, consisting of the exact center (node *a*) and the extreme corner (node *f*), and four other locations (*b*, *c*, *d*, and *e*) which represent transitional locations from center to corner. As another angle, the resulting spatial distributions of $L_i(d)$ for all 225 nodes by selected ranges of $L_i(d)$ for $d = 5.0$, 9.9, and 15.0 (range A, B, and C in Fig. 2a, respectively) are portrayed in Fig. 2b–d, respectively. There are several key insights to be noted from the simulation experiment. First, based on the trajectories of nodes in Fig. 2a, each node reaches the maximal $L_i(d)$ (i.e., ceiling point that the bandwidth covers all other nodes, ≅ 7.92 on the y-axis in this experiment) at different bandwidths. Notice that node a corresponds to the location that needs the smallest bandwidth ($d = 9.9$) to cover all nodes, whereas node f is the location that needs the greatest bandwidth at $d = 19.8$ to include all other nodes in computing $L_i(d)$. The other four nodes reach the maximal point in the order of $b < c < d < e$, which is clearly dependent upon their locations and the number of neighborhood nodes j and their d_{ij}. Second, the experiments inform that range of $L_i(d)$ values among nodes becomes wider until the bandwidth d reaches around the first ceiling point where the gaps among the $L_i(d)$ are most effectively distinguished given the pattern of nodes in the study area (Fig. 2c). Based on this observation, we define the ideal bandwidth named d_{opt}, which is the best bandwidth as a criterion of D-SIP of each node using the following Equations (6) and (7).

$$d_{\text{opt}} = \min \left\{ d_i^{\min} | 1 \leq i \leq n \right\} \tag{6}$$

$$d_i^{\min} = \min \left\{ d | \max_d \left(L_i(d) \right) \right\} \tag{7}$$

where d_{opt}: the ideal bandwidth of all $L_i(d)$, and $d_i^{\min}$: the minimum bandwidth that is maximized $L_i(d)$ for all i.

It is generally observed that a node located around the center of space reaches the ceiling point first (refer to Fig. 1a) and its $d_i^{\min}$ is likely to be d_{opt}. Specifically, Equation (6) specifies that d_{opt} is defined as the minimum value among $d_i^{\min}$, the smallest bandwidth of $L_i(d)$ that is stipulated by equation (7) for all nodes i through pre-processing in a GIS environment. Once d_{opt} is determined, the $L_i(d_{\text{opt}})$ is computed for all nodes, and we will use these values as criterion values to determine if the node i with $L_i(d_{\text{opt}})$ is classified as either an essential or non-essential decision variable. We define $L_i(d_{\text{opt}})$ as $L_i^{D\text{-}SIP}$ using Equation (8), where d_{opt} plays an important role that makes the $L_i(d)$ values of nodes most stretched in the distribution of them. Within this distribution, the $L_i^{D\text{-}SIP}$ values for essential decision variables form distinctive clusters, providing a robust criterion for their conservation while eliminating non-essential decision variables in the p-dispersion problems.

$$L_i^{D\text{-}SIP} = L_i\left(d_{\text{opt}}\right) = \sqrt{\frac{A \sum_{j=1}^{n} k_{ij}}{\pi(n-1)}} \tag{8}$$

where $L_i^{D\text{-}SIP}$: the local K-function value at node i with the ideal bandwidth d_{opt}, and k_{ij}: 1 if $d_{ij} \leq d_{\text{opt}}$, or 0 otherwise.

We hypothesize that the decision variables of the optimal solutions are strongly associated with the $L_i^{D\text{-}SIP}$. In other words, if a distinct cluster of $L_i^{D\text{-}SIP}$ of optimal solutions can be identified, the range of $L_i^{D\text{-}SIP}$ values in the cluster may serve as a criterion to determine decision variables as essential or non-essential variables in solving the instance. Then, of critical concern is how to articulate the *collective dominance* of optimal solutions with the behavior of their $L_i^{D\text{-}SIP}$, which is explored by numerical experiments.

Design of simulation experiments

To demystify how the $L_i^{D\text{-}SIP}$ leverages the determination of the optimal solutions of p-dispersion problems, we designed intensive simulation experiments by different spatial patterns of nodes in a study area – which are classified with (a) center-clustered, (b) random, and (c) edge-clustered pattern. Then, these instances are generated using different probability distributions of the coordinates of nodes – normal, uniform, and beta distributions with a setting of $\alpha = 0.5$ and $\beta = 0.5$ (i.e., *Beta* (0.5, 0.5)[i]), respectively. The first simulation experiment is designed for

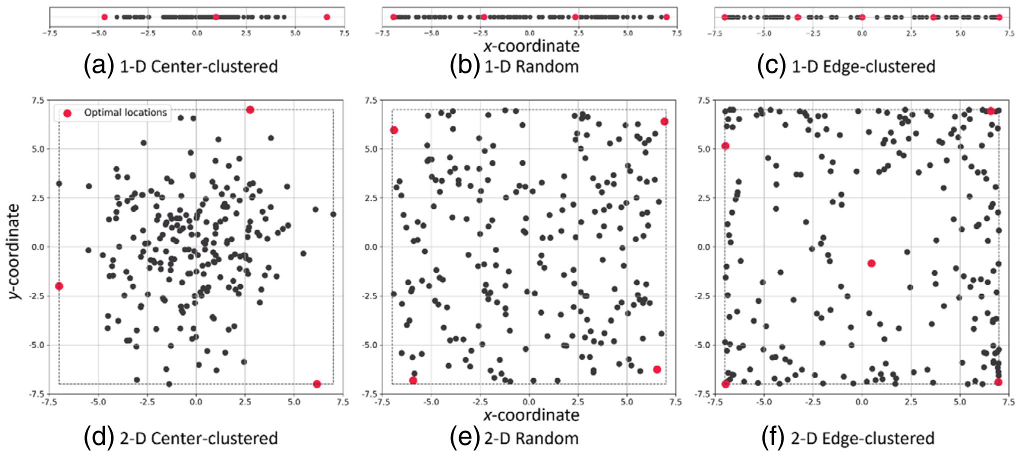

Figure 3. Examples of different spatial point patterns for simulation experiments in one-dimensional (a, b, c) and two-dimensional spaces (d, e, f). The red dots in the figures depict the optimal dispersion locations of each sample instance for $p=3$, 4, and 5 for center-clustered, random, and edge-clustered, respectively.

the instances that are generated in a line-shaped space (Fig. 3a–c) with 100 nodes, and a square-shaped research space (Fig. 3d–f) with 225 nodes. The former and the latter represent one-dimensional and two-dimensional spaces, respectively. We illustrate the optimal locations of the *p*-dispersion problems for $p=2$, 3, and 5 in the figures to enhance understanding of how the solutions are generally distributed (depicted as red dots in the figures). Given the problem size of the nodes and computational times required to confirm the exact optimal solutions by the conventional MIP form of the *p*-dispersion problems, the range of $p=2$–5 was tested. To draw a generalization of the simulation results, the optimal solutions from generated 1,000 replications for each type of the spatial patterns were summarized using general tendencies. Further, clustered patterns of both the collection of the optimal solutions and their D-SIPs were analyzed. Note that although solving the *p*-dispersion problem for $p=2$ instances is straightforward, we intentionally included these instances to demonstrate the behavior of the D-SIPs.

Based on the simulation results, we will discuss the key findings from the distribution of the D-SIPs for the optimal solutions of the *p*-dispersion problems. As previously discussed, non-essential decision variables identified by the D-SIP can be safely eliminated from the original model without compromising optimality. The criteria determining essential or non-essential decision variables will be derived from the D-SIP distribution. Section 4.4 will provide a detailed procedure for the identification and elimination of non-essential decision variables to construct SI-dispersion models from the original *p*-dispersion problem. Computational experiments for the SI-dispersion models will be presented to demonstrate improved computational efficiency and optimality of the model.

Results

D-SIP histogram: Collective dominance of optimal solutions in one-dimensional dispersion problems

We begin with simulation experiments for a one-dimensional space. The interpretation of the behavior of D-SIP in one-dimensional space is straightforward because the optimal locations of

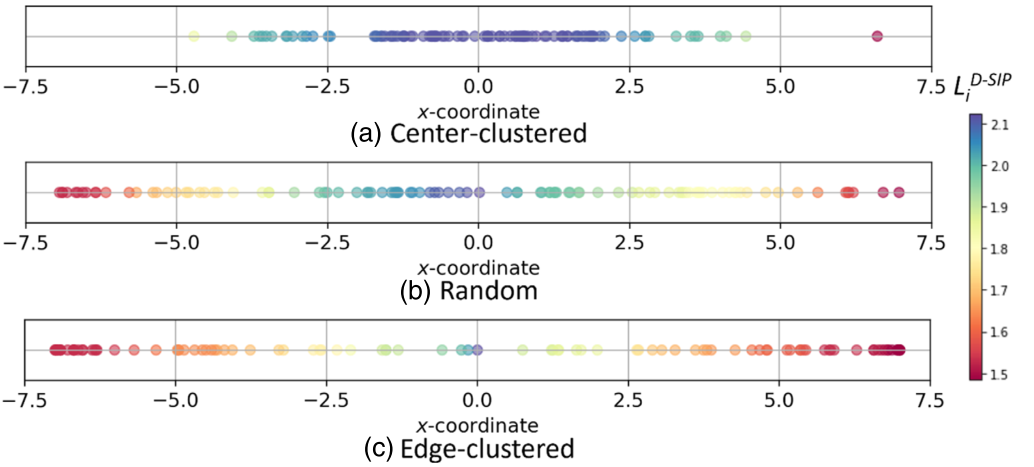

Figure 4. Distribution of $L_i^{D\text{-}SIP}$ values by three types of spatial pattern in a one-dimensional space.

p nodes are determined solely by the distances among nodes on a *single* line. The findings can also serve as a foundation to understand the behavior of the solutions in a two-dimensional space.

Fig. 4 shows that the behavior of $L_i^{D\text{-}SIP}$ values across three different types of spatial distributions of nodes is consistent, demonstrating that higher $L_i^{D\text{-}SIP}$ values (blue dots) are concentrated in the center area, while lower values (red dots) are found in the peripheral areas of the study area. These spatial patterns of $L_i^{D\text{-}SIP}$ values are governed by the characteristics of the edge effect from the local K-function $L_i(d)$. In general, in areas further away from the center, nodes tend to have lower $L_i^{D\text{-}SIP}$ values, as they have relatively fewer neighboring nodes within the specified bandwidth, compared to the nodes in the center of the space. In other words, the edge effect produces unique spatial information about the D-SIP among nodes in the space.

To better describe the behavior of the optimal solutions related to the distribution of $L_i^{D\text{-}SIP}$ values, we use a D-SIP histogram. Fig. 5 provides an example of D-SIP histograms for the case of $p = 3$ under the random point pattern in a one-dimensional space. The histogram depicts the frequency of the optimal solutions (y-axis) with the range of $L_i^{D\text{-}SIP}$ values (x-axis) and their corresponding locations of the optimal solutions (portrayed on the top of the histogram) drawn from 1,000 iterations for each point pattern, projecting the locations of the optimal solutions into the distribution of L_i in a histogram frame. Figs. 6–8 are the complete results of the D-SIP histograms by three different types of spatial patterns with $p = 2$–5.

Two observations are worthy to note from the D-SIP histograms. First, as clearly demonstrated in Fig. 5, there is strong evidence that the $L_i^{D\text{-}SIP}$ values of the nodes in the optimal solutions are clustered in the histogram. In this case, the $L_i^{D\text{-}SIP}$ of all optimal solutions falls within the range of two clusters [1.20, 1.77] or [2.10, 2.13]. This implies that the decision variables (Y_i) with $L_i^{D\text{-}SIP}$ values within these two clusters tend to be essential for optimal solutions, while the rest of them distant from these clusters are likely to be non-essential. We refer to the specific clusters of optimal solutions identified by $L_i^{D\text{-}SIP}$ as the *collective dominance* of optimal solutions. In general, the collective dominance of optimal solutions may exhibit a bell-shaped (see the dotted left box) distribution, or an isolated high-frequency pillar with a narrow range of $L_i^{D\text{-}SIP}$ (see the dotted right box), which is observed also for odd values of p

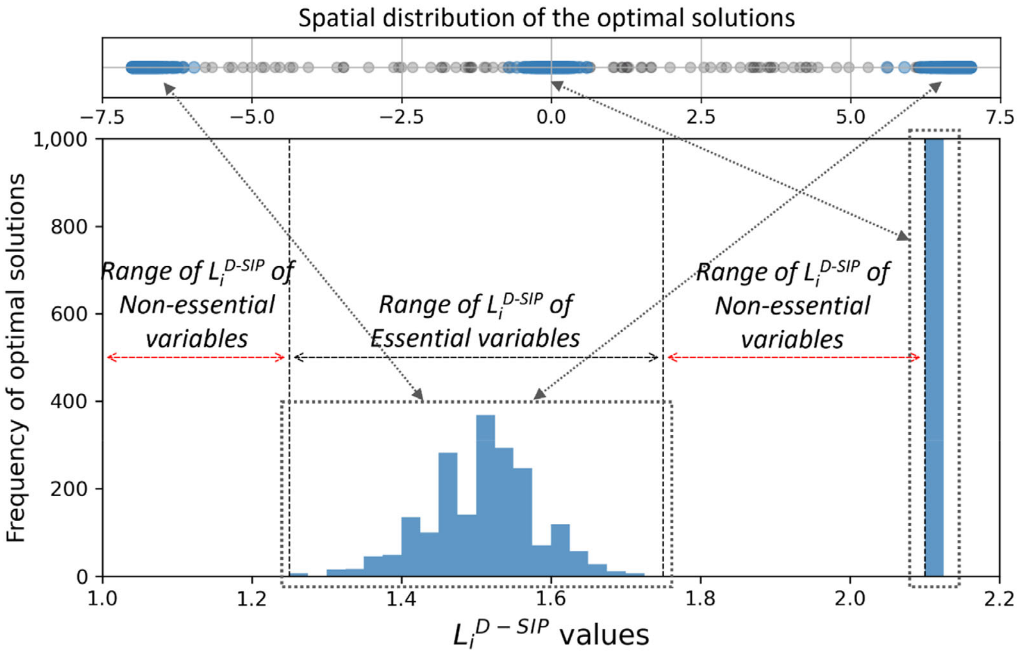

Figure 5. D-SIP histograms: The distribution of $L_i^{D\text{-}SIP}$ of the optimal solutions in a one-dimensional space: The case of $p=3$ under the random point pattern. Grey dots in the map on the top are an instance of the random point pattern to depict the distribution of optimal solutions clearly.

(=3 and 5 in Figs. 6–8, for example), strongly indicating the presence of an optimal solution in the center of the area.

Secondly, the behavior of collective dominance of the optimal solutions is also influenced by the types of spatial patterns of nodes and p as well observed in Figs. 6–8 where the shapes of collective dominances are diverse although the collective dominance is observed across all spatial patterns and different p. Note that the distribution of these collective dominances varies depending on the types of spatial patterns of nodes and the value of p (i.e., odd/even number). For example, the more the location of optimal solutions is dispersed (though clustered), the wider shape of collective dominances is observed. For example, in a center-clustered spatial pattern (Fig. 6), the less intense collective dominance(s) (i.e., widely-spread histograms) are observed. In contrast, the tendency of concentration is pronounced in random spatial patterns (Fig. 7), and much more prominent in the edge-clustered patterns in the D-SIP histogram (Fig. 8), presenting distinct collective dominance. In essence, the presence of collective dominance, if clearly presented, can serve as a promising criterion in effectively narrowing down the feasible solution space in the MIP formulation by eliminating unnecessary decision variables or conserving potentially optimal solutions of Y_i from the constraints (3) and (4), as well as the objective function.

D-SIP histogram: Collective dominance of optimal solutions in two-dimensional dispersion problems

The simulation experiments in a two-dimensional space confirm that this association holds. In other words, if a cluster of $L_i^{D\text{-}SIP}$ values in the D-SIP histogram is clearly identifiable in

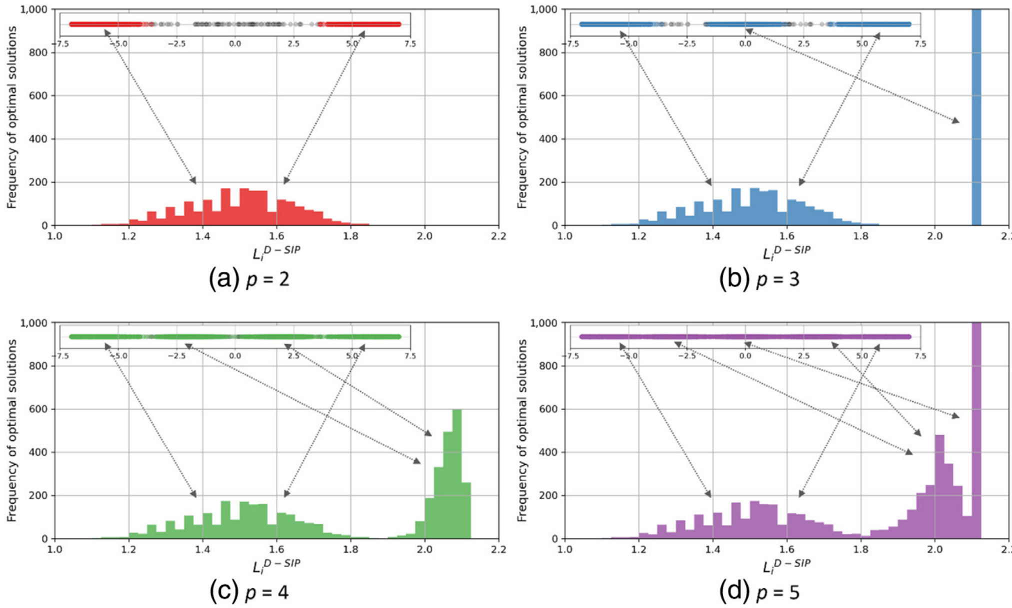

Figure 6. D-SIP histogram: The distributions of the optimal solutions to the one-dimensional center-clustered point pattern.

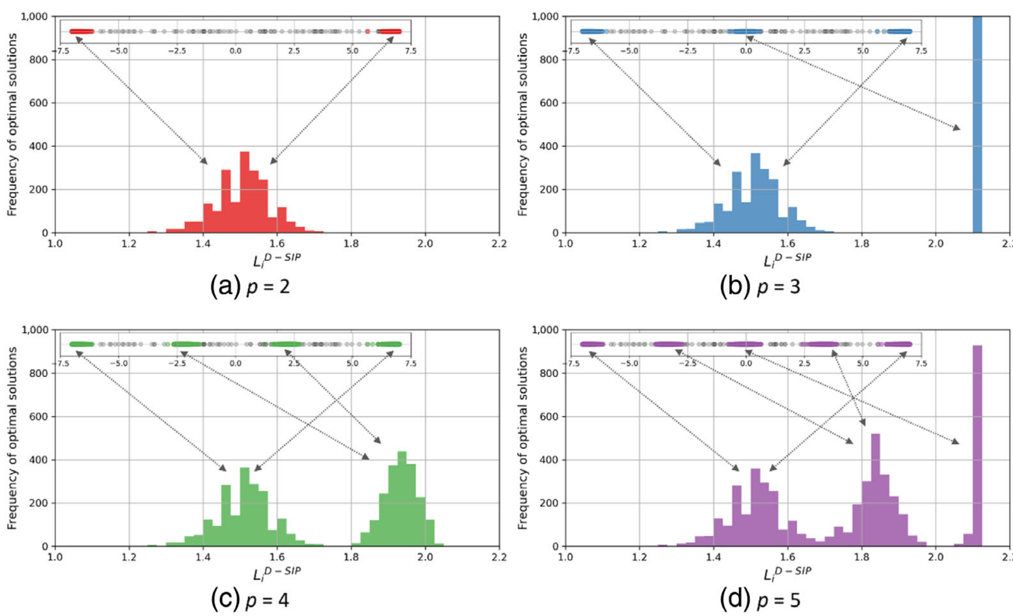

Figure 7. D-SIP histograms: The distributions of the optimal solutions to the one-dimensional random point pattern.

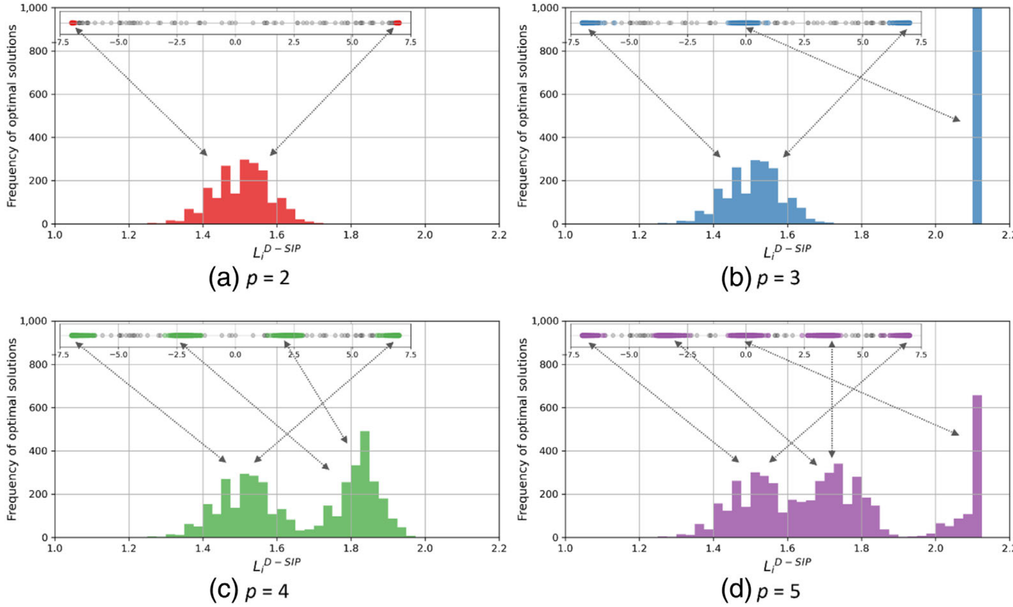

Figure 8. D-SIP histograms: The distributions of the optimal solutions to the one-dimensional edge-clustered point pattern.

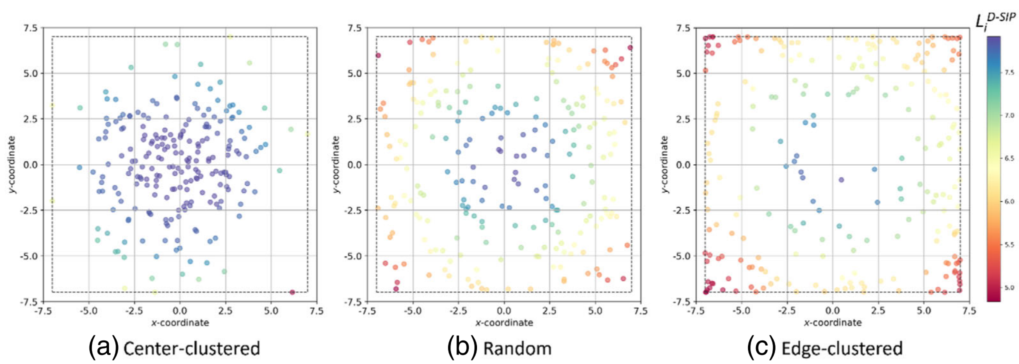

Figure 9. Distribution of $L_i^{D\text{-}SIP}$ values on instances by spatial patterns of nodes in s two-dimensional space.

a two-dimensional space, nodes with $L_i^{D\text{-}SIP}$ values that fall within the collective dominance can be considered as potential candidates for the optimal solutions. Fig. 9, which depicts the distributions of $L_i^{D\text{-}SIP}$ values on instances of different spatial patterns of nodes in a two-dimensional space, confirms the findings observed in the one-dimensional space also hold identical in a two-dimensional space. The clustering tendency of higher $L_i^{D\text{-}SIP}$ values around the center and the dispersion of lower $L_i^{D\text{-}SIP}$ values around the edges or corners of the space persist in the two-dimensional space.

Fig. 10 illustrates the D-SIP histogram and the location of the optimal solutions in the two-dimensional research space for the case of random point patterns with $p = 5$. Analogous to the results of the one-dimensional experiments, it is evident that the D-SIP histogram reveals

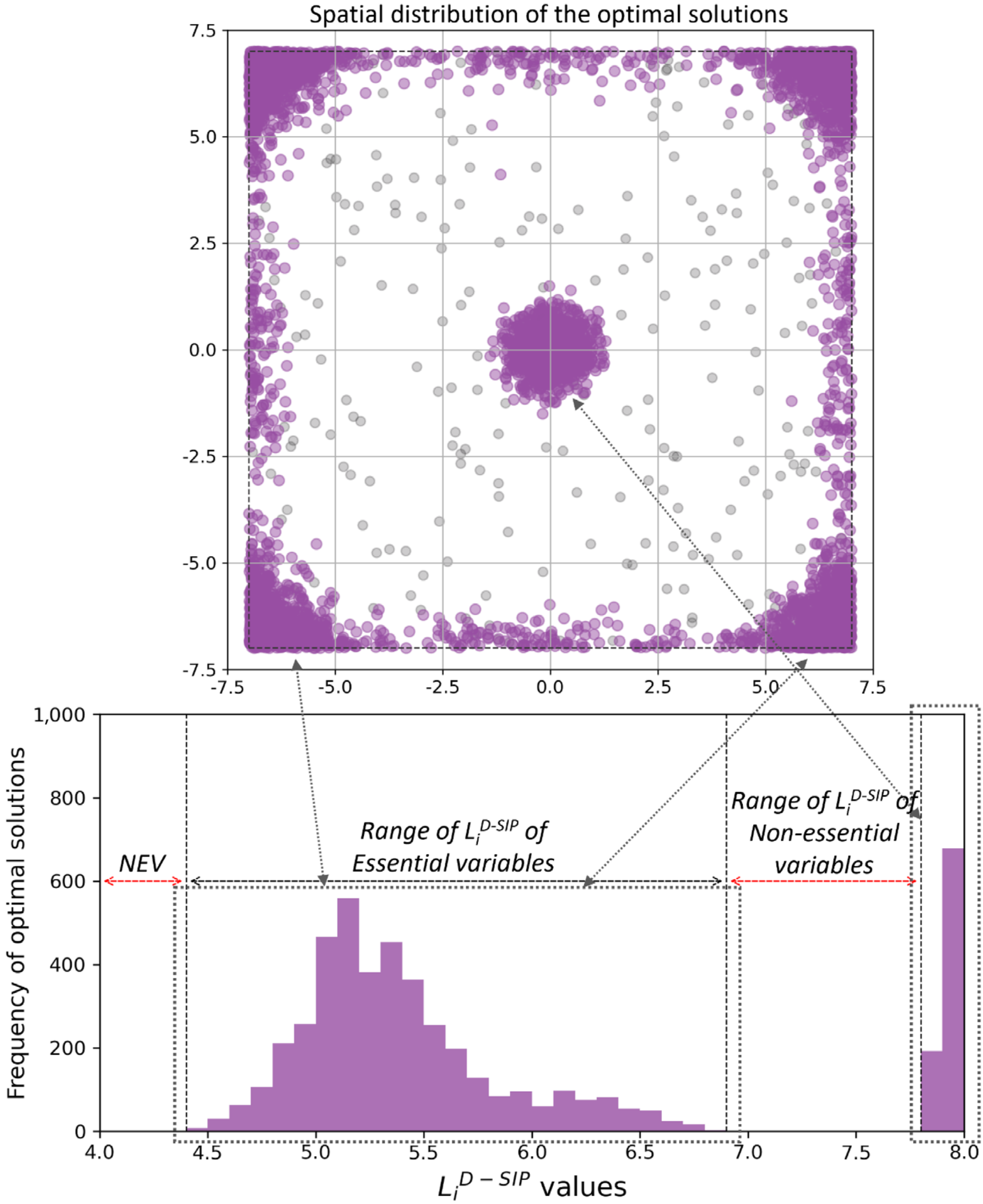

Figure 10. D-SIP histograms: The distribution of $L_i^{D\text{-}SIP}$ of the optimal solutions in a two-dimensional space: The case of $p = 5$ under the random point pattern. Grey dots in the map on the top are an instance of the random point pattern to depict the distribution of optimal solutions clearly; NEV is an abbreviation of Non-Essential Variables.

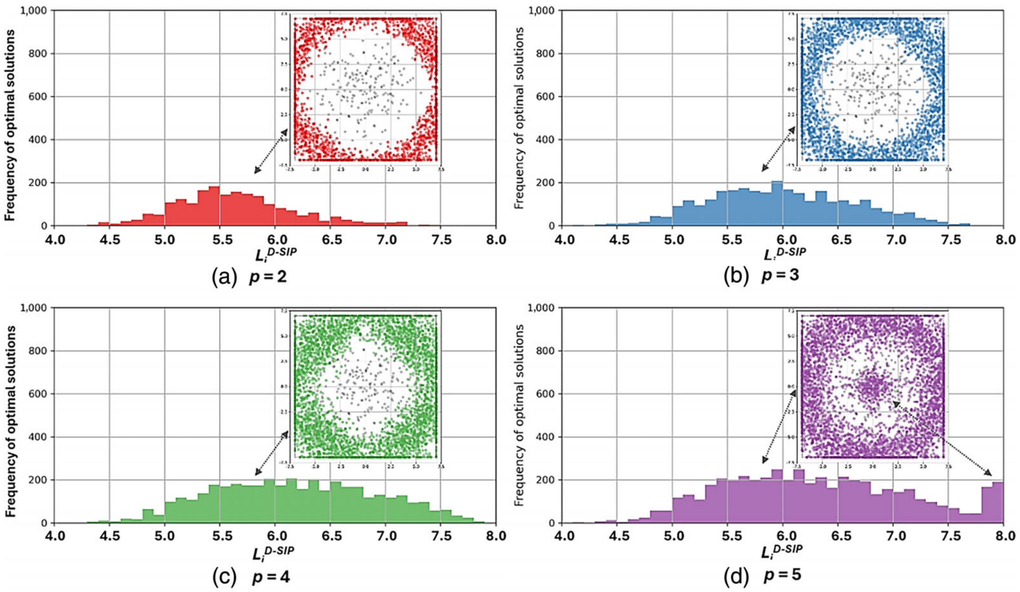

Figure 11. D-SIP histograms: The distributions of the optimal solutions to the two-dimensional center-clustered point pattern.

the optimal solutions are clustered in the histogram as a form of collective dominances and they are clearly delineated with specific ranges. In this case, the $L_i^{D\text{-}SIP}$ values of the decision variables for optimal solutions fall within the range of either [4.34, 6.99] or [7.82, 7.92], while the decision variables not relevant to the optimal solutions are outside these ranges. Another observation to be noted is that the significance of collective dominance is governed by types of underlying spatial point patterns. By examining Figs. 11–13 together, the collective dominance of the D-SIP is more clearly observed in the random (Fig. 12) and the edge-clustered pattern (Fig. 13), compared to the center-clustered point pattern (Fig. 11). In sum, it should be underscored that most of the areas in the research spaces of random or edge-clustered patterns are the fields of non-collective dominance where a considerable number of decision variables in the fields would not be essential in finding optimal solutions and, thereby, can be safely removed from the MIP models with little risk of degrading the optimally dispersed solution.

Note that there are two distinct forms of collective dominance observed in the two-dimensional space, which are also shown in the one-dimensional space experiments. Generally, a bell-shaped distribution with a specific range of $L_i^{D\text{-}SIP}$ values, or a pillar-type (multi-modal) distribution, where extremely high $L_i^{D\text{-}SIP}$ values are densely clustered, is displayed. The latter form is particularly well observed when the optimal solution is located near the center of the study area, which is often the case for odd values of p, as consistently noticed in Figs. 11d, 12d, and 13d. However, compared to the one-dimensional experiments, the collective dominance in the two-dimensional space is generally less intense due to the elevated spatial dimensionality. Nevertheless, the underlying principle of the D-SIP remains consistent, demonstrating its effectiveness in determining the optimal solutions for the p-dispersion problems in the two-dimensional space.

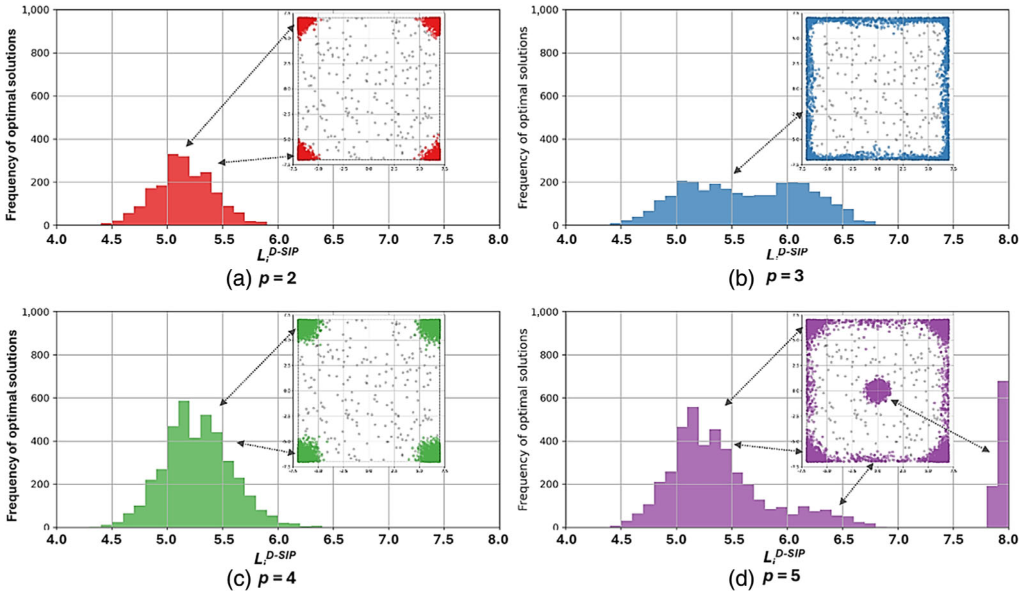

Figure 12. D-SIP histograms: The distributions of the optimal solutions to the two-dimensional random point pattern.

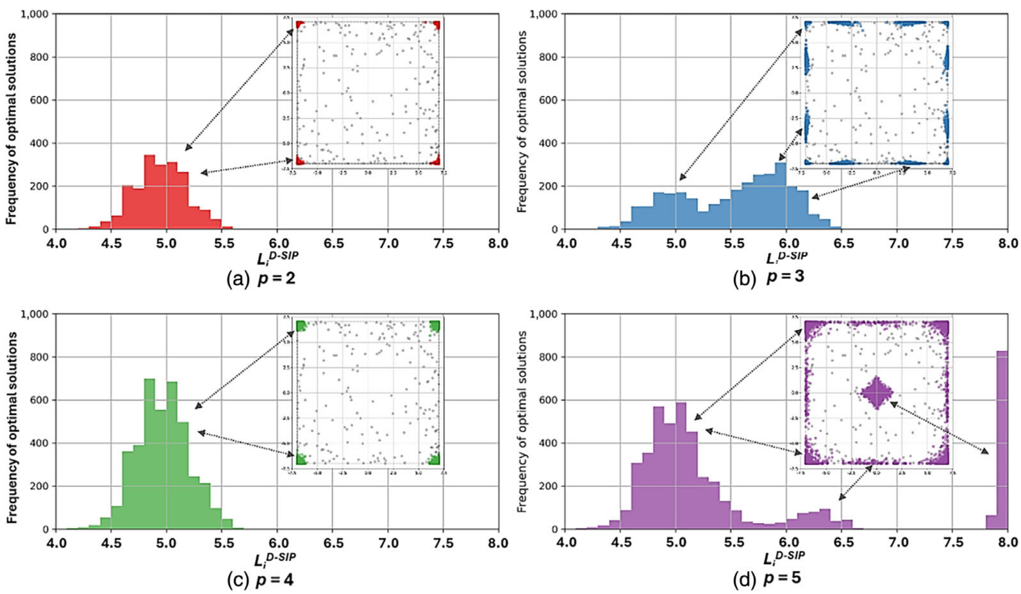

Figure 13. D-SIP histograms: The distributions of the optimal solutions to the two-dimensional edge-clustered point pattern.

Key findings of D-SIP

Based on the observations from the experiments, several noteworthy findings have been identified. First, the collective dominance for the optimal solutions is consistently observed in both one-dimensional and two-dimensional experiments, indicating the behavior of optimal solutions can be spatially informed via the D-SIP histograms. The simulation experiments reveal that collective dominances are outcomes derived from the spatial association between the relative locations of the nodes and their *K*-function values. If identified, the collective dominance of $L_i^{D\text{-}SIP}$ values on the D-SIP histograms represents a set of essential decision variables for the optimal solutions of the *p*-dispersion problem.

Second, the D-SIP of the underlying point pattern strongly influences the behavior of determining the location of the optimal solutions. As shown in both one- and two-dimensional experiments, specific areas are delineated where the optimal solutions are more distinctively found. Additionally, the level of cluster concentration required for collective dominance varies with the types of underlying point patterns. The more the input nodes are edge-clustered in a particular form, the clearer collective dominance of the optional solutions is observed. In contrast, where the input nodes are center-clustered, then the collective dominance tends to be difficult to determine because the center-clustered point pattern is less conducive to forming distinct clusters of optimal solutions. This implies that *p*-dispersion problems characterized by specific types of spatial point patterns, such as edge-clustered, would benefit more from utilizing the D-SIP to solve the problem.

Finally, the findings suggest that the D-SIP can be used as a criterion to slim the original MIP model of the *p*-dispersion problem by discerning non-essential variables from the model that fall outside the range of collective dominance. In essence, a MIP model reduced by removing non-essential decision variables is expected to outperform the original one, especially considering the situation when exact solutions are crucially required but limited due to the problem size. The next section presents how to build the SI-dispersion models, focusing on the elimination procedure of non-essential variables based on the D-SIP.

Building SI-dispersion model

To demonstrate the feasibility of the SI-dispersion model, we used a cumulative percentage of rank-based criteria to eliminate non-essential decision variables in a robust manner. Fig. 14 illustrates the procedures for constructing the SI-dispersion models. Fig. 14a shows a set of curved plots for $p = 2$, 3, 4, and 5, with cumulative percentage distributions of the rank of $L_i^{D\text{-}SIP}$ values of nodes (on the *y*-axis) ordered by rank (on the *x*-axis) for the random point pattern example. Each curved plot for *p* is created by transforming the $L_i^{D\text{-}SIP}$ values into a cumulative percentage of rank (Fig. 14b). This transformation procedure is a way of standardization to the ranges of the original $L_i^{D\text{-}SIP}$ values which vary with instance (types of point patterns, number of demands, and *p*). Additionally, converting original values into ranks and calculating their cumulative percentage helps determine the cut-off area of $L_i^{D\text{-}SIP}$ values (gray areas in the diagrams).

In detail, to rank the $L_i^{D\text{-}SIP}$ value of each optimal solution in a given instance, we sorted the values in ascending order, such that solutions with lower $L_i^{D\text{-}SIP}$ values were assigned lower ranks, and then changed with the percentage of rank over the total number of candidate nodes in an instance. The cumulative plots shown in Fig. 14a provided the basis for setting the criteria to remove non-essential variables from the original *p*-dispersion model. In this analysis, non-essential decision variables are easily identified as the variables that fell within the vertical

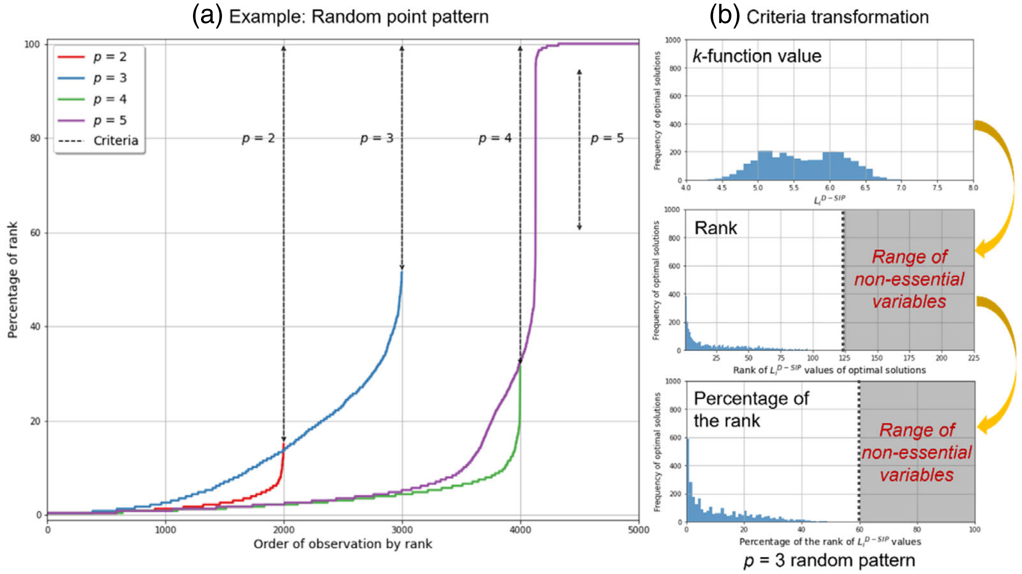

Figure 14. Illustration of the elimination criteria for constructing the SI-dispersion models. The percentage of the rank is calculated by the following: $\frac{Rank}{N} * 100$, where N is the total number of nodes.

ranges (see the vertical black dotted lines on the cumulative plots as the criteria in the diagram), as these variables are clearly non-essential. However, we made an exception for a special case exemplified in $p = 5$ on purpose, as the plot creates a continuous curved line with a "plateau" at the end, which may indicate a collective dominance of optimal solutions can be found in the section with the plateau. For these cases, we used a criterion based on visual inspection and removed decision variables within a range of 60%–90% ranks, which is empirically acceptable as a "conservative" cut-off. Once we define the reduced set of the decision variables as S^R based on the elimination criteria, the constraints of the MIP formulation of the SI-dispersion model are re-formulated as follows, while the objective function of the model remains identical:

Subject to

$$\sum_{i \in S^R} Y_i = p \tag{9}$$

$$D \leq d_{ij} + M\left(2 - Y_i - Y_j\right) \quad \forall i, j \in S^R, \;\; j > i \tag{10}$$

$$Y_i \in \{0, 1\} \quad \forall i \in S^R \tag{11}$$

where S^R: the set of the decision variables determined by the cumulative rank-based elimination criterion.

Throughout constraints (5), (6), and (7), the decision variables that satisfy the elimination criterion are only included in the model in a set of S^R. Consequently, the number of constraints of the SI-dispersion models is fewer than the original p-dispersion models. To investigate the capability of our D-SIP, we conducted additional experiments to compare the performance between the original p-dispersion problem and the SI-dispersion model. We generated 1,000 instances for each of the three spatial point patterns. For each instance, we solved both the original

Table 1. Results of the Numerical Experiments for the SI *p*-Dispersion Models ($p = 2$–5)

p	# of nodes in the SI models*	# of the optimal solutions**	Averaged ratio of optimality gap (%)***	Reduction of solution time (%)
(a) Center-clustered				
2	67	1000 (100%)	0.00	93.07
3	135	1000 (100%)	0.00	73.04
4	67	987 (98.7%)	0.02	94.18
5	158	956 (95.6%)	0.04	55.49
(b) Random				
2	67	1000 (100%)	0.00	91.17
3	135	999 (99.9%)	0.00	67.52
4	67	999 (99.9%)	0.00	95.57
5	158	999 (99.9%)	0.00	55.95
(c) Edge-clustered				
2	67	998 (99.8%)	0.00	91.62
3	135	962 (96.2%)	0.01	74.50
4	67	993 (99.3%)	0.00	96.79
5	158	935 (93.5%)	0.09	35.60

*The number of nodes in the original model is 225.
**1,000 instances generated for each pattern, totaling 12,000 instances.
***Optimality gap is defined as the difference between the best solution derived from mixed integer programming (MIP_{opt}) and the upper bound obtained when the instance is solved under relaxed conditions using linear programming (LP_{opt}).

p-dispersion problems and their SI-dispersion models using the commercial solver ILOG CPLEX 12.8 on an Intel Core i7-4790 3.60GHz machine with 16GB of RAM to compare the results.

Table 1 presents the results of the SI-dispersion models by different point patterns and provides a comparison of the optimal solutions with the optimal solutions obtained from the original *p*-dispersion models. The comparison is conducted using a set of criteria, which includes the rates of obtaining exact solutions, the averaged ratio of gaps (%), and the reduction of solution times (%). The first column, "the number of the optimal solutions," presents the effectiveness of the SI-dispersion models in finding the exact optimal solutions across 12,000 instances from our experiments. The second column displays the averaged gaps as a % of differences between the optimal solutions of two dispersion models. The third column shows the % of reduction in solution times achieved by the SI-dispersion models compared to the original models.

Based on the results, several noteworthy implications emerge. First, the SI-dispersion models found the exact optimal solutions for nearly all instances (<99.9%, out of 12,000 instances), though the lowest percentages are found in the $p = 5$ edge-clustered patterns (93.5%). However, the average gaps (%) for those cases are extremely small (0.04%–0.09%), and the average percentage gaps between the original and the SI-dispersion models are less than 0.1% for all the different spatial patterns of nodes and all of p, which are often considered negligible. In our investigation of the mismatch of optimal solutions between the two groups of models, we found that the reasons are twofold: data input errors, specifically relating to the precision of coordinates, and the presence of less clearly defined criteria decisions. Second, it should be underscored that the solution times of the SI-dispersion models are notable in all instances.

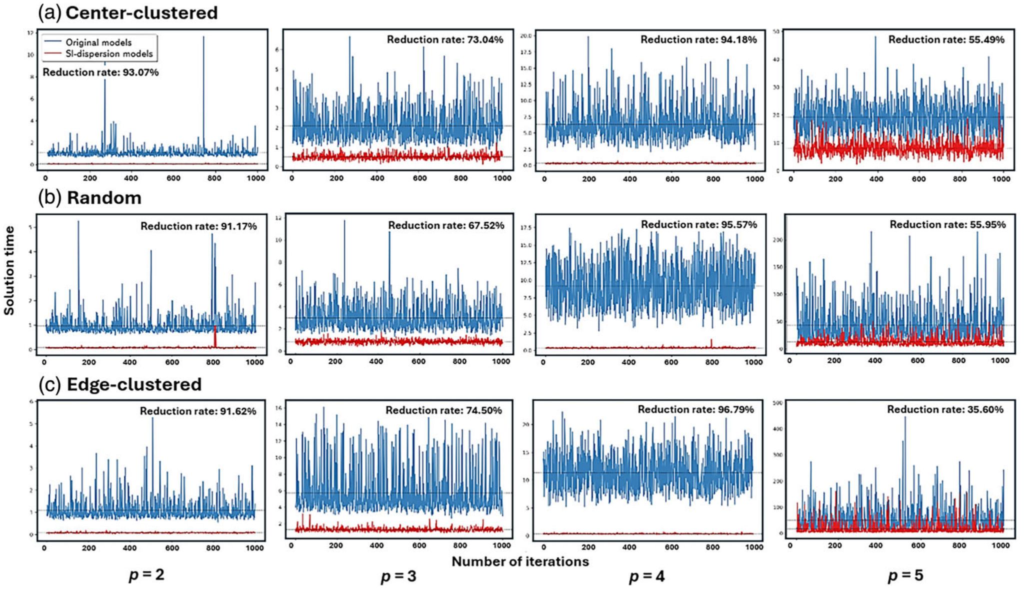

Figure 15. Solution times comparison by underlying point patterns and the number of p. The x-axis represents the number of iterations, and the y-axis represents the solution time (s) of each instance.

While the extent of reduction times varies with p, the average percentage of reduced time is about 70% across all instances, and up to 97% for specific instances (e.g., edge-clustered pattern with $p = 4$). Fig. 15 compares the solution times of the original models (blue lines), and the SI dispersion models (red lines). Considering that the solution times using the original p-dispersion models ranged from a few seconds to a few minutes (approximately 8 min), the SI-dispersion models consistently outperformed them across all the instances. Most instances were solved within several seconds, with the worst performance taking only 161 s. Particularly noteworthy is the exceptional performance of the SI-dispersion models with an even number of p (2 and 4) instances, demonstrating significant solution times reduction (>90%) with a minor compromise in the quality of the solutions for only a few instances still provided exact optimal solutions in approximately 99% of instances.

However, it should also be noted that the efficacy of the SI-dispersion model might deteriorate if the reduced number of decision variables and constraints remains large and it does not lead to a considerable reduction in the complexity of the problem. Fig. 16 provides a concise example illustrating the comparison of solution times between the SI-dispersion model and the original model across different sizes of n by n regular grid (n varies from 5 to 80 with the interval of 5) when $p = 2$. Not surprisingly, the solution times of the original p-dispersion problems rapidly increase beyond approximately a 30 by 30 grid (900 nodes). In contrast, the solution times of the SI-dispersion models remain remarkably short until the size reaches 55 by 55 (3,025 nodes). However, beyond 70 by 70 (4,900 nodes), the solution times of the SI-dispersion models also increase quickly. This simple illustration implies that there would be a specific zone of the size of the problems where the SI-dispersion modeling approach can effectively outperform the original problems, even though the challenge does not necessarily limit the capability of a D-SIP approach.

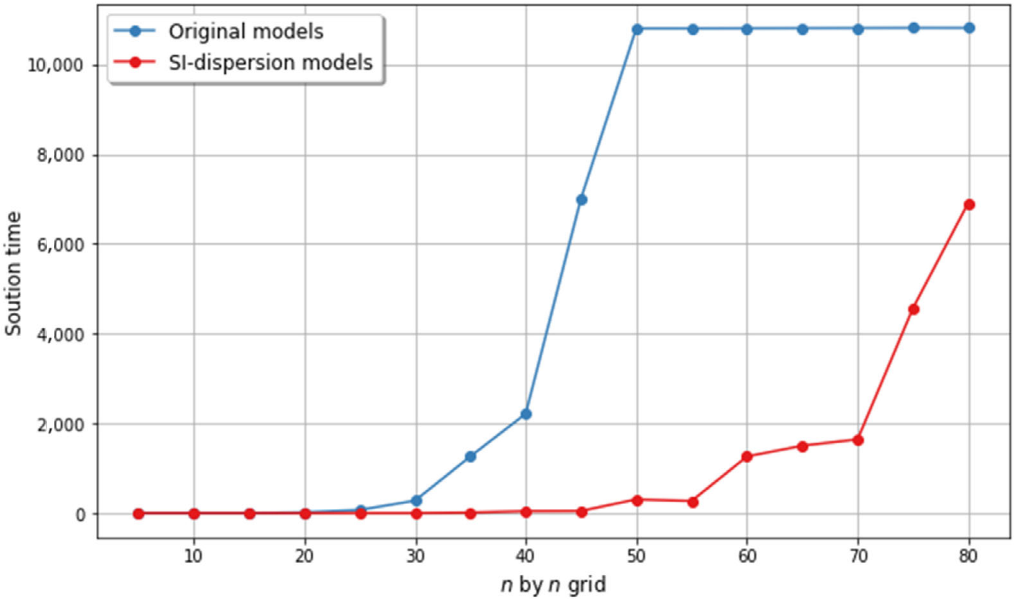

Figure 16. Solution times comparison by different problem sizes (regular grid point pattern, $p = 2$). The maximum solution time is limited to 3 h (10,800 s) in the CPLEX solver for illustration purposes.

The comparative analysis between the two models reveals that the effectiveness of the SI-dispersion model varies based on different point patterns and the number of *p*. As depicted in Table 1, optimal solution quality and time reduction are maximized when the number of *p* is smaller, particularly under random or center-clustered point patterns. Among the three different point patterns, random point patterns consistently yield the most reliable and efficient results in terms of both optimality and computational performance. Conversely, edge-clustered point patterns exhibit comparatively less efficient outcomes. We expanded tests using instances with higher values of p (=6–9) for 1,200 instances (4 $p \times 3$ types $\times 100$ instances). These results consistently maintain significantly small optimality gaps, averaging at 0.73% across all instances with up to 44% reduction in solution times, demonstrating the validity of the SI-dispersion model. However, the extended results also indicate that benefits from the SI-dispersion model may diminish. Particularly, it is observed when $p \geq 10$ in our instances where the separation distances among open nodes in a square space become too restricted, hindering the emergence of the distinct collective dominance for essential decision variables, which is critical to ensure the model's performance. Given the stringent conditions of our experiments, further research is warranted to examine the efficacy of the SI-dispersion model for empirical data, encompassing a wider range of distances among nodes.

Concluding remarks and future research

The main contributions of this research are threefold. First, we introduce the D-SIP approach for solving the classical *p*-dispersion problem from a different methodological perspective by uncovering the relationship between the D-SIP and the behavior of the optimal solutions to different spatial patterns of the input nodes and proving the superiority of the SI-dispersion models over the original p-dispersion models in MIP form. Up to our knowledge, this approach has received little attention, although there has been discussion on its potential through the concept of *collective dominance* derived from the behavior of a spatial optimization problem, accompanied by the elaboration of criteria to identify it. Simulation experiments revealed that the use of D-SIP is rationalized to build efficient exact, or almost near-optimal solution methods for the p-dispersion problems, significantly improving its solvability and applicability.

Second, our findings could allude to more in-depth subjects, creating latent conjectures between the D-SIP and the applications that utilize the p-dispersion problems through advancing solution approaches using different solution strategies. These strategies include a more precise method for eliminating the redundant decision variables or maintaining the essential decision variables without loss of generality, both of which are assisted by the D-SIP. Examples include developing heuristic algorithms that incorporate the idea of the D-SIP to improve their performance in initial solution strategies or searching frames (e.g., meta-heuristics), and expanding the D-SIP with other advanced data-driven searching methods such as machine learning, to enhance the search paths towards optimal solutions for extremely large instances.

Finally, in view of real applications, more diverse settings of data should be tested. The experiments in this research were conducted in a controlled setting to minimize the influence of external factors. The point patterns used had coordinates with symmetrical distributions around the center point of the space, which is a challenging environment for MIP solvers to identify optimal solutions. Exploring the properties of the D-SIP on asymmetrical point patterns with different parameter settings, or in irregularly shaped spaces such as long rectangular spaces would be more realistic in applications.

Endnote

1 Two parameters for a beta distribution, α and β, determine the shape of the probability density function (PDF). In the case of $\alpha = 0.5$ and $\beta = 0.5$, the PDF of the beta distribution forms a U-shape, that the very low values (near 0) and high values (near 1) have a high probability while medium values have a low probability. So, the coordinates with the *Beta(0.5, 0.5)* probability distribution form an "edge-clustered" spatial point pattern, in which many nodes are located at the periphery area of the space, while relatively few nodes are located at the center of the space.

References

Contardo, C. (2020). "Decremental Clustering for the Solution of p-Dispersion Problems to Proven Optimality." *INFORMS Journal on Optimization* 2(2), 134–44.

Chandrasekaran, R., and A. Daughety. (1981). "Location on Tree Networks: p-Centre and n-Dispersion Problems." *Mathematics of Operations Research* 6(1), 50–7.

Chandrasekaran, R., and A. Tamir. (1982). "Polynomially Bounded Algorithms for Locating p-Centers on a Tree." *Mathematical Programming* 22, 304–15.

Chaudhry, S. S., S. T. McCormick, and I. D. Moon. (1986). "Locating Independent Facilities with Maximum Weight: Greedy Heuristics." *Omega* 14(5), 383–9.

Church, R. L. (2003). "COBRA: A New Formulation of the Classic p-Median Location Problem." *Annals of Operations Research* 122, 103–20.

Curtin, K. M., and R. L. Church. (2006). "A Family of Location Models for Multiple-Type Discrete Dispersion." *Geographical Analysis* 38, 248–70.

Curtin, K. M., and R. L. Church. (2007). "Optimal Dispersion and Central Places." *Journal of Geographical Systems* 9(2), 167–87.

Daskin, M. S. (2013). *Network and Discrete Location: Models, Algorithms, and Applications*, 2nd ed. New York: Wiley.

Erkut, E. (1990). “The Discrete *p*-Dispersion Problem.” *Journal of Operational Research* 46(1), 48–60.

Getis, A., and J. Franklin. (1987). “Second Order Analysis of Mapped Point Patterns.” *Ecology* 68, 473–7.

Ghosh, J. B. (1996). “Computational Aspects of the Maximum Diversity Problem.” *Operations Research Letters* 19(4), 175–81.

Griffith, D. A. (2021). “Articulating Spatial Statistics and Spatial Optimization Relationships: Expanding the Relevance of Statistics.” *Stats* 4(4), 850–67.

Griffith, D. A., Y. Chun, and H. Kim. (2022). “Spatial Autocorrelation Informed Approaches to Solving Location-Allocation Problems.” *Spatial Statistics* 50, 100612.

Griffith, D. A., Y. Chun, and H. Kim. (2023). “The Majority Theorem for the Single ($p = 1$) Median Problem and Local Spatial Autocorrelation.” *Geographical Analysis* 55(1), 107–24.

Kim, H., Y. Chun, and D. A. Griffith. (2019). Spatial Autocorrelation for Solving *p*-Median Problem, *Annual Meeting of American Association of Geographers (AAG)*, April 5, 2019, Washington D.C.

Kuby, M. J. (1987). “Programming Models for Facility Dispersion: The *p*-Dispersion and Maxisum Dispersion Problems.” *Geographical Analysis* 19(4), 315–29.

Kuo, C. C., F. Glover, and K. S. Dhir. (1993). “Analyzing and Modeling the Maximum Diversity Problem by Zero-One Programming.” *Decision Sciences* 24(6), 1171–85.

Lei, T. L., and R. L. Church. (2015). “On the Unified Dispersion Problem: Efficient Formulations and Exact Algorithms.” *European Journal of Operational Research* 241(3), 622–30.

Mei, X., K. M. Curtin, D. F. Turner, N. M. Waters, and M. Rice. (2022). “Approximating the Length of Vehicle Routing Problem Solutions Using Complementary Spatial Information.” *Geographical Analysis* 55(1), 125–54. https://doi.org/10.1111/gean.12322.

O’Sullivan, D., and D. Unwin. (2010). *Geographic Information Analysis*. New Jersey: Wiley.

Parreño, F., R. Álvarez-Valdés, and R. Martí. (2021). “Measuring Diversity, A Review and an Empirical Analysis.” *European Journal of Operational Research* 289(2), 515–32.

Pisinger, D. (2006). “Upper Bounds and Exact Algorithms for *p*-Dispersion Problems.” *Computers & Operations Research* 33, 1380–98.

Ripley, B. D. (1976). “The Second-Order Analysis of Stationary Point Processes.” *Journal of Applied Probability* 13(2), 255–66.

Ripley, B. D. (1977). “Modeling spatial patterns.” *Journal of the Royal Statistical Society: Series B (Methodological)* 39(2), 172–92.

Sayah, D., and S. Irnich. (2017). “A New Compact Formulation for the Discrete *p*-Dispersion Problem.” *European Journal of Operational Research* 256, 62–7.

Sayyady, F., and Y. Fathi. (2016). “An Integer Programming Approach for Solving the *p*-Dispersion Problem.” *European Journal of Operational Research* 253, 216–25.

Shier, D. R. (1977). “A Min-Max Theorem for p-Center Problems on a Tree.” *Transportation Science* 11(3), 243–52.

Tansel, B. C., R. L. Francis, T. J. Lowe, and M. L. Chen. (1982). “Duality and Distance Constraints for the Nonlinear p-Center Problem and Covering Problem on a Tree Network.” *Operations Research* 30(4), 725–44.